

Accepted Manuscript

SnO₂/ZnO composite dye-sensitized solar cells with graphene-based counter electrodes

K. Robinson, G.R.A. Kumara, R.J.G.L.R. Kumara, E.N. Jayaweera, R.M.G. Rajapakse

PII: S1566-1199(18)30040-5

DOI: [10.1016/j.orgel.2018.01.040](https://doi.org/10.1016/j.orgel.2018.01.040)

Reference: ORGELE 4512

To appear in: *Organic Electronics*

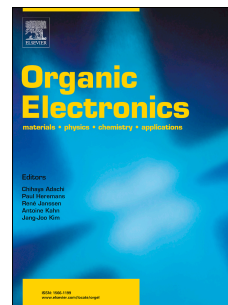
Received Date: 18 December 2017

Revised Date: 15 January 2018

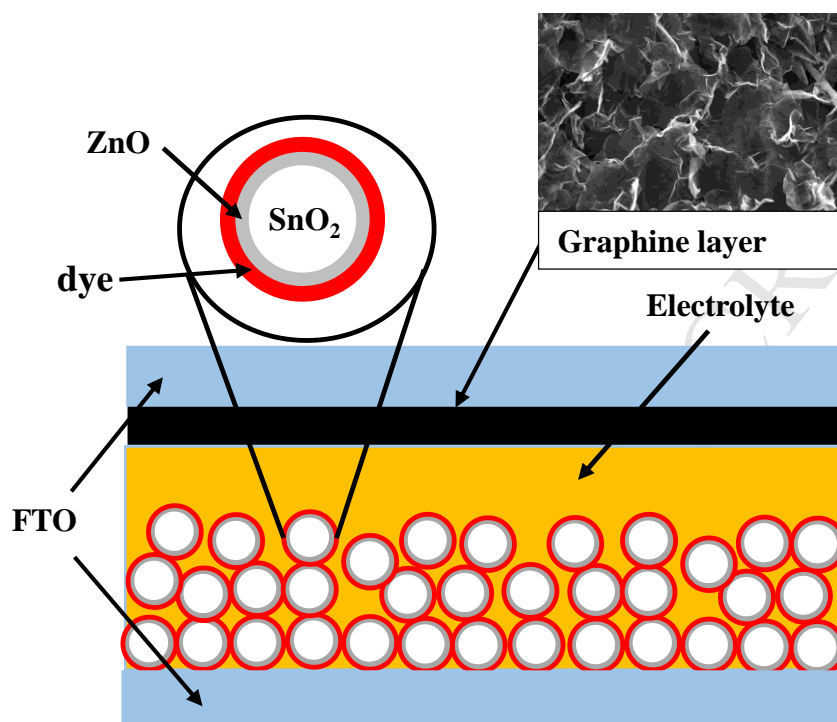
Accepted Date: 28 January 2018

Please cite this article as: K. Robinson, G.R.A. Kumara, R.J.G.L.R. Kumara, E.N. Jayaweera, R.M.G. Rajapakse, SnO₂/ZnO composite dye-sensitized solar cells with graphene-based counter electrodes, *Organic Electronics* (2018), doi: [10.1016/j.orgel.2018.01.040](https://doi.org/10.1016/j.orgel.2018.01.040).

This is a PDF file of an unedited manuscript that has been accepted for publication. As a service to our customers we are providing this early version of the manuscript. The manuscript will undergo copyediting, typesetting, and review of the resulting proof before it is published in its final form. Please note that during the production process errors may be discovered which could affect the content, and all legal disclaimers that apply to the journal pertain.



Graphical abstract



SnO₂/ZnO Composite Dye-Sensitized Solar Cells with Graphene-based Counter Electrodes

K. Robinson¹, G. R.A. Kumara^{1, 2,*}, R. J. G. L.R. Kumara¹, E. N. Jayaweera¹ and R. M. G. Rajapakse^{1,3}

¹Postgraduate Institute of Science, University of Peradeniya, Peradeniya, 20400, Sri Lanka

²National Institute of Fundamental Studies, Hantana Road, Kandy, 20000, Sri Lanka

³Department of Chemistry, University of Peradeniya, Peradeniya, 20400, Sri Lanka

Abstract

We have pioneered in developing dye-sensitized solar cells with interconnected nanoparticles of semiconductors other than TiO₂ and we found that despite impressive properties of semiconducting materials such as ZnO and SnO₂ which should theoretically give better performances than those based on TiO₂, they give quite inferior performances and we explained this unprecedented fact by considering faster recombination of injected electrons in the latter semiconductor nanoparticles than those in TiO₂ nanoparticles. To circumvent this problem, we introduced a novel technology in which we covered the surfaces of interconnected nanoparticles of SnO₂ by an ultra-thin layer of a wide band-gap semiconductor or an insulator where the thickness of the layer is ~1 nm or less such that electron injection from the excited dye molecules to the conduction band of the semiconductor nanoparticles is possible but injected electrons are incapable of penetrating the insulating barrier layer. In this way, we were able to suppress recombination significantly and such composite film based dye-sensitized solar cells gave efficiencies comparable to those based on TiO₂ nanoparticles. We then realized that platinum used in dye-sensitized solar cell counter electrodes accounts for nearly 40% of the cost of these solar cells and hence limits their practical application. We then worked on alternative materials and found that carbon based counter electrodes can be tailored to give efficiencies closer to those of Pt counter electrode based solar cells. In extending this study we now worked on graphene as counter electrode material for composite SnO₂/ZnO dye-sensitized solar cells. We report in this manuscript the optimizations of this low-cost counter electrode based dye-sensitized solar cell to give performance closer to those of expensive platinum based counterparts.

Key Words:

Dye- sensitized solar cells; Inter connected nano-particles; Counter electrodes; Graphene; Pt

1. Introduction

In our previous publications, we documented the development of dye-sensitized solar cells using interconnected SnO₂ nanoparticles covered with thin shells of ZnO (SnO₂/ZnO) as dye-absorbing and electron transporting materials where we have replaced usually used interconnected TiO₂ nanoparticles with interconnected SnO₂/ZnO nanoparticles [1-3]. Our choice of SnO₂ instead of TiO₂ was stemmed from several reasons. First, it has been found that the structural, electronic, and optical properties in SnO₂ epitaxial thin films can be tuned

by applying strain on the structure. Particularly, the optical band gap of SnO₂ can be significantly reduced with increasing the tensile strain in the bc plane [4, 5]. Density functional calculations have revealed that the narrowing of the optical band gap of SnO₂ under tensile strain is due to weakening of bonding and anti-bonding split resulting from the disorder of SnO₆ octahedra [6]. It has also been reported that biaxial strain is more effective than uniaxial strain in reducing the band gap of SnO₂. It has been shown that the optical band gap of SnO₂ epitaxial thin films can be reduced by 0.7 eV from 3.6 eV this decreasing to 2.9 eV where SnO₂ is now capable of absorbing in the visible range. Secondly, SnO₂ is a good choice of semiconductor since it is chemically a highly stable material that is insoluble even in highly corrosive chemicals such as acids, bases and strongly oxidizing and reducing agents and has a conduction band (CB) bottom below the lowest unoccupied molecular orbital (LUMO) energy levels of many dyes that are commonly used in dye-sensitized solar cells (DSCs) thus enabling faster transfer of excited electrons in the LUMO levels of excited dye molecules to the bottom of the CB of SnO₂ nanoparticles. Thirdly, SnO₂ nanoparticles can be fused with FTO layer in the working electrode due to their chemical similarities where FTO is lightly fluoride-doped SnO₂. As such, electrons that are transported along the interconnected SnO₂ nanoparticles can be transferred to FTO layer without any potential energy barrier thus giving improved fill factor for the solar cells fabricated. Fourthly, the electron mobility in SnO₂ nanoparticles is much higher than that in TiO₂ nanoparticles with identical size and shape thus giving faster electron mobility along SnO₂ nanoparticles than that along TiO₂ nanoparticles. Despite all these advantages, we found that the overall photon-to-electron conversion efficiency with SnO₂ based DSCs are much inferior than that of TiO₂ based ones under otherwise identical compositions and conditions. We explained this by considering the rates of recombination of electrons in the two materials. The electrons injected to the SnO₂ particles move faster than those in TiO₂ particles and thus reach the surfaces of particles more frequently in SnO₂ than that in TiO₂. Once electrons reach the particle surfaces they are prone to react with oxidized dye molecules that are attached to the surface of particles and any tri-iodide ions that are at the vicinity of the particles. As such, although electrons are injected satisfactorily and are able to transport towards FTO back contact faster than that does by interconnected TiO₂ nanoparticles, electron losses due to recombination is higher in SnO₂ based DSCs than those in TiO₂ based ones thus giving inferior DSC performances by SnO₂ based ones [7,8]. In order to circumvent this problem, we introduced a novel method where we used an ultra-thin coating of a high band gap semiconductor or an insulator to cover the particle surfaces of SnO₂ [9-11]. This thin layer is only a few atomic layer in thickness thus giving ~1 nm thick coating covering the entire exposed surfaces of interconnected nanoparticles of SnO₂ [12-13]. Dye molecules are actually attached to the outer surface of the ultra-thin coat but the thickness is so small that electrons excited on the LUMO levels of the dye molecules can be transferred to SnO₂ nanoparticles in a ballistic manner since electron wave function can penetrate ~1 nm distance [14]. These electrons are energetic also and hence they are capable of moving fast along the interconnected SnO₂ nanoparticles. Once injected, electrons are in a lower energy state than those when present in the LUMO levels of the dye molecules and hence they are unable to come to the outer surface of the thin coat thus preventing the encounter with oxidized dye molecules and I₃⁻ ions for recombination losses. As such, we were able to improve the DSC performance of SnO₂ based DSCs by introducing an ultra-thin shell of ZnO or MgO or CaCO₃ etc.

Although, all these DSCs give impressive conversion efficiencies, their practical application is limited by the high cost of the counter electrode (CE) material used. The usual counter electrode is made with lightly platinized FTO glass and the major cost of the entire device is due to platinum that is used in this counter electrode. However, platinum is perhaps the best electro-catalyst for triiodide reduction though the corrosive triiodide ions can etch the platinum particles present on the CE surface. If platinum can be replaced by a cheaper material and the DSCs function as good as platinum CE based ones then of course these DSCs are more viable for practical applications. With this aim in mind, we studied graphene counter electrode based N-719 dye coated SnO₂/ZnO DSCs with usual iodide/triiodide liquid electrolyte and studied the performance by optimizing with respect to the graphene counter electrode properties and thickness of the graphene layer and in this manuscript we detail them giving quantitative data of DSC performances comparing it with that of DSC based on Pt CE. We have already reported the success of using counter electrodes based on graphite/graphene products with DSCs [15-17]. This success in using low-cost counter electrodes to reduce the cost of production of DSCs by nearly 40% stemmed us to work further on graphene counter electrode based DSCs and this is one such another study and several more studies will follow in subsequent publications.

2. Experimental

2.1. Preparation of the dye-coated SnO₂/ZnO composite film working electrode

3.0 mL of SnO₂ colloid (Alfar Aesar, 15% SnO₂ colloidal in H₂O) was mixed with 10 drops of acetic acid (Sigma Aldrich, 99.8 %) and 0.060 g of ZnO powder (Kanto Chemicals, Japan) and ground well to obtain a transparent paste. Then, 5 drops of Triton X100 (Wako Chemicals, Japan) was added and ultra-sonicated for 5 minutes to obtain a fine dispersion sol. Thereafter, it was sprayed on pre-heated (150 °C) FTO surface and sintered at 500 °C. It was then allowed to cool down to 80 °C and immersed in N719 (Ruthenizer 535-bisTBA FULL NAME, purchased from Solaronix, Switzerland) dye solution containing 0.30 mM N719 dye dissolved in a solution of t-butanol and acetonitrile in 1:1 volume ratio for 12 hours. The electrode was then rinsed with acetonitrile and allowed to air-dry.

2.2. Fabrication of graphene counter electrode

0.015 g of carboxymethyl cellulose (CMC, Sigma Aldrich) in 25.0 ml of de-ionized water was stirred thoroughly to obtain a clear solution. 150 mg of graphene powder (United nanotech Innovations, India) was then added and stirred well by ultra-sonication to obtain a fine graphene dispersion. It was then heated at 100 °C to evaporate some water to obtain a graphene paste. The graphene paste thus prepared was applied on FTO glass plate using screen printing method and sintered at 300 °C for 30 min. The amount of CMC, sintering temperature and thickness of the graphene film were varied to obtain optimum parameters to get best DSC performance.

2.3. Construction of the cell and studying DSC performance

The dye sensitized solar cells were fabricated as usual by sandwiching the electrolyte solution containing I₃/I redox couple between working electrode and graphene counter electrode. The DSC performances were studied using a PECcell-L01 solar simulator coupled to a Keithley (2400 model) multimeter, under 1.5 AM illumination. Kinetic parameters of the DSCs were evaluated by AC impedance Spectroscopy (Potentiostat Autolab)

3. Results and discussion

As for optimizing the graphene-based CE, different morphologies of graphene layers on FTO were prepared by mixing 150 mg of graphene with different amounts of CMC and applying them separately on FTO surfaces and heat-treating at 300 °C to give an approximate thickness of 50 μm on FTO surface and the solar cell performances of the usual liquid electrolyte-based DSCs constructed using these graphene-based CEs were measured and the data obtained are tabulated in Table 1.

Table 1

Solar cell performances of the usual liquid electrolyte-based DSCs constructed using graphene-based CEs which was prepared using 150 mg graphene and different amounts of carboxymethyl cellulose treated at 300 °C to give an approximate thickness of 50 μm on FTO surface.

Counter electrode		V_{OC}/V	J_{sc} (mA/cm ²)	FF	η (%)
GN-00 CMC	00 mg	0.610	12.3	0.61	4.62
GN-05 CMC	05 mg	0.628	12.9	0.58	4.73
GN-10 CMC	10 mg	0.633	13.0	0.62	5.11
GN-15 CMC	15 mg	0.644	13.4	0.62	5.35
GN-20 CMC	20 mg	0.653	12.0	0.65	5.11
GN-25 CMC	25 mg	0.656	11.6	0.63	4.83

It is interesting to note that the morphology of the graphene layer has a distinct effect on the open circuit voltage, V_{OC} , where V_{OC} is steadily increasing when the amount of CMC used in the CE preparation is increased. When the amount of CMC in the graphene-CMC mixture is increased and the pastes thus prepared were applied on FTO surfaces and heat-treated to burn away CMC the CEs thus formed have voids in places where CMC was present. This gives porous structure for the graphene layer on FTO surfaces. As the amount of the CMC is increased the resulting graphene layer on FTO will be more and more porous and hence the CE can be properly wetted by the liquid electrolyte. This gives high surface area for the reduction of tri-iodide ions to iodide ions. The efficient generation of iodide ions at the CE contributes directly to the improved performance of DSCs. Therefore, it is possible that efficient regeneration of iodide ions will efficiently react with oxidized dye molecules thus decreasing the possibility of recombination of electrons injected to SnO₂/ZnO nanoparticles with oxidized dye molecules and tri-iodide ions. This will result in upward shift of the Fermi level of the electrons injected to SnO₂/ZnO nanoparticles. As such, even if the potential of the I₃⁻/I⁻ reduction on graphene-based CE is independent of its morphology the V_{OC} would increase due to up-ward shift of the Fermi level. It is also possible that increase in V_{OC} due to different amounts used in graphene-based CE preparation may be indicating that the potential of the I₃⁻/I⁻ reduction on graphene-based CE is dependent on the history of CE preparation

which gives porous structure for the graphene film. Higher the porosity higher the active surface area of CE material and hence higher its electro-catalytic activity. Anyhow, the important outcome of this experiment is that higher the porosity of the graphene layer in the graphene-based CE the higher the V_{OC} in usual liquid electrolyte-based DSCs.

On the same account, one would expect to observe steady increase in J_{SC} also as the porosity is increased. However, data in Table 1 show that J_{SC} is indeed increasing up to a maximum value from which it is decreasing as the porosity of the graphene layer in the CE is increased. The initial increase in J_{SC} with CE porosity is clear since efficient removal of oxidized dye molecules by efficiently formed iodide ions at the CE would decrease the recombination of injected electrons with oxidized dye molecules and tri-iodide ions. This would increase the number of electrons collected by the device and hence the J_{SC} . However, as the porosity is increased the electrical conductivity of the CE layer would become less. The decreased electrical conductivity of the CE would add increased series resistance to the DSC thus decreasing the J_{SC} . Therefore, it is clear that there is an optimum value for the porosity of the graphene layer on FTO in the CE to give the highest DSC performance. Since the FF of the DSCs is independent from the history of CE preparation, i.e., porosity of the graphene layer on FTO, it is likely that graphene adheres well on FTO regardless of its porosity. As such, electrons that have come to the FTO layer on the CE can be effectively transferred to the graphene layer regardless of the porosity of the graphene layer.

In order to optimize the heat-treatment temperature of graphene-based CE preparation, the CMC amount was kept at 15 mg since it gives the highest efficiency as indicated in Table 1 and the CE was prepared using 150 mg graphene, 15 mg of CMC mixture applied on FTO heat treating at different temperatures. The CEs thus prepared were used in usual liquid electrolyte-based DSCs and their performances are depicted in Table 2.

Table 2

Solar Cell Parameters of liquid-based dye-sensitized solar cells prepared by using counter electrodes which were prepared using 150 mg graphene, 15 mg carboxymethyl cellulose mixture applied on FTO surfaces which were heat-treated at different temperatures.

Counter electrode	V_{oc}/V	J_{sc} (mA/cm ²)	FF	η (%)
GN- 200 °C	0.668	11.9	0.57	4.57
GN- 250 °C	0.658	12.2	0.59	4.77
GN- 300 °C	0.644	13.5	0.62	5.41
GN- 350 °C	0.649	12.5	0.60	4.90
GN- 400 °C	0.706	10.5	0.62	4.56

Results indicate that there is no particular trend in the variation of individual solar cell parameters with respect to the temperature of heat treatment. The best efficiency of 5.41% is obtained when the counter electrode was prepared by heat treating it at 300 °C and therefore further optimizations were carried out by heat treating the CE at this temperature. Using 150 mg of graphene and 15 mg of CMC, the paste of which applied on the FTO surface heat treated at 300 °C to obtain different thicknesses of the active layer on CE were used in DSCs and their performances are tabulated in Table 3.

Table 3

Solar Cell performance of the graphene-based dye-sensitized solar cells as a function of the counter electrode thickness.

Counter electrode	V_{OC}/V	J_{SC} (mA/cm^2)	FF	η (%)
GN- 20 μm	0.663	12.3	0.55	4.55
GN- 30 μm	0.657	12.5	0.57	4.72
GN- 40 μm	0.647	12.7	0.61	5.01
GN- 50 μm	0.643	12.8	0.64	5.34
GN- 60 μm	0.643	13.8	0.62	5.50
GN- 70 μm	0.646	12.6	0.65	5.36
GN- 80 μm	0.639	12.5	0.64	5.13

As the thickness of the CE is increased the effect on V_{OC} seems to be very small or slightly decreasing as the thickness is increased. This may be due to increased resistance of the CE. This is further manifested in the J_{SC} values which increase up to $13.8 mA/cm^2$ at $60 \mu m$ thickness and then decreases as the thickness is further increased. Increased thickness of the porous graphene layer would give increased surface area for the tri-iodide reduction which would increase the current density. However, the opposing effect due to increased resistance of the CE would come into play as the thickness is increased. As such, the observed trend can be expected. Fill factor seems to increase and then level off around 0.64. This is probably due to proper binding of the graphene layer on FTO as the thickness is increased which would better facilitate the electron transfer from FTO to graphene layer when the latter is tightly bound to the former. The collective effect on the conversion efficiency is that it increases up to $60 \mu m$ thickness of the graphene layer on CE and then decreases. With all these optimized conditions, the highest efficiency of 5.50% was obtained.

In order to compare the efficiency of the SnO_2/ZnO based DSCs with graphene counter electrode and usual lightly platinized FTO-Cr counter electrode the efficiency of the former with optimized conditions was compared with that of the latter. The J-V performances of the two DSCs under otherwise identical conditions are shown in Figure 1 and the solar cell parameters extracted from these J-V curves are tabulated in Table 4. It is interesting to note that SnO_2/ZnO based DSCs also give such an impressive conversion efficiency of 7.17% when Pt-based CE is used. The conversion efficiency is slightly lower when graphene based CE is used and the best value obtained here is 5.50%. This decrease in efficiency could be compensated by the huge decrease in the cost of fabrication of the DSCs. As indicated earlier, although DSCs stand out to be the low-cost alternatives to standard silicon solar cells the majority of the cost of DSCs is due to the cost of platinum used in the CE. Replacement of platinum by graphene which can be derived from low-cost graphite could be a way forward for practical applications of DSCs. It is clear from the data given in Table 4 that all three solar cell parameters are lesser for the graphene CE based DSC than those for Pt CE based DSC. In order to investigate the difference in the conversion efficiencies, we carried out AC impedance spectroscopic studies of the two CEs of the DSCs.

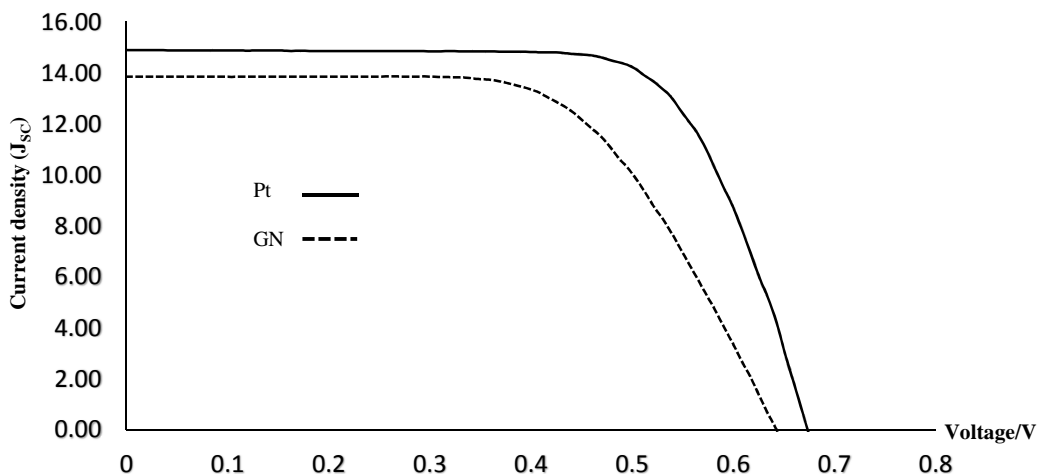


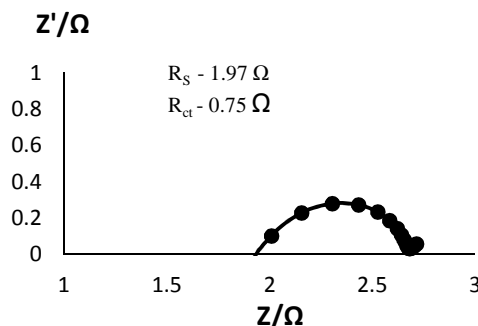
Fig.1. J-V curves for SnO₂/ZnO dye-sensitized solar cells with graphene-based and Pt-based counter electrodes.

Table 4

Comparison of the DSC performance of the usual liquid electrolyte based SnO₂/ZnO DSC with graphene and Pt counter electrodes.

Counter electrode	V _{OC} /V	J _{SC} (mA/cm ²)	FF	η (%)
Pt	0.687	15.0	0.69	7.17
GN	0.643	13.8	0.62	5.50

The Nyquist plots of the AC impedance spectra shown in Figure 2 clearly indicate that both the series resistance R_s and the charge transport resistance R_{ct} , are higher when graphene based CE is used instead of Pt-based CE. This is because Pt is a better electrocatalyst for triiodide reduction than graphene. This explains lower conversion efficiency observed for DSCS when graphene based CE is used instead of Pt-based ones. Nevertheless, the difference is small and the advantage associated with low-cost graphene derived from local graphite can outweigh the lower performance and hence as far as practical applications are concerned, graphene based ones are more viable than Pt-based ones.



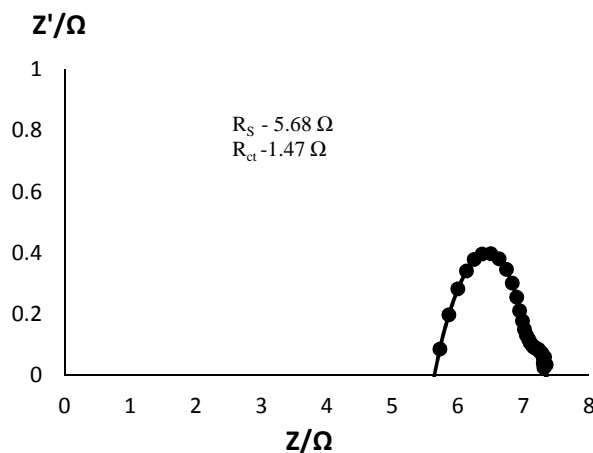


Fig. 2. The Nyquist plots of AC impedance spectra of (a) Pt CE based DSC and (b) Graphene CE based DSC.

4. Conclusion

Graphene counter electrode based DSCs utilizing SnO₂/ZnO interconnected nanoparticle charge transport layer instead of TiO₂ nanoparticle layer were prepared and optimized with respect to counter electrode preparation conditions and DSC performance studied. The best DSC gives 5.5% conversion efficiency as opposed to 7.1% efficiency obtained similar DSCs with Pt-based counter electrodes. The lower performance is explained by considering the sluggish kinetics of triiodide reduction on graphene when compared to faster reduction of triiodide ions on platinum as indicated by AC impedance studies. However, the difference is not too large and low-cost of graphene based DSCs might overcome the lower performance for practical applications.

References

1. K. Tennakone, G. R. R. A. Kumara, I. R. M. Kottegoda, V. P. S. Perera, An Efficient Dye-sensitized Photoelectrochemical Solar Cell made from Oxides of Tin and Zinc, *Chem. Comm.* (1999) 15-16.
2. G. R. A. Kumara, K. Tennakone, I. R. M. Kottegoda, P. K. M. Bandaranayake, A. Konno, M. Okuya, S. Kaneko, K. Murakami, Efficient Dye-sensitized Photoelectrochemical Cells made from Nanocrystalline Tin(IV) oxide–Zinc oxide Composite Films, *Semicond. Sci. Technol.* 18 (2003) 312-318.
3. W.M.N.M.B. Wanninayake, K. Premaratne, R.M.G. Rajapakse, Highly Efficient Dye-Sensitized Solar Cells Based on Synthesized SnO₂ Nanoparticles *J. Nanomaterials.* (2016) 1- 8.
4. W. Zhou, Y. Liu, Y. Yang, P. Wu, Band Gap Engineering of SnO₂ by Epitaxial Strain: Experimental and Theoretical Investigations, *J. Phys. Chem. C* 118 (2014) 6448–6453.

5. O. Mounkachi, E. Salmani, M. Lakhal, H. Ez-Zahraouy, M. Hamedoun, M. Benaissa, A.Kara, A.Ennaoui, A.Benyoussef, Band-gap engineering of SnO₂, Sol. Energy Mater . Sol. Cells (2015), <http://dx.doi.org/10.1016/j.solmat.2015.09.062i>
6. W. Zhou, Y. Liu, Y. Yang, Ping Wu, Band Gap Engineering of SnO₂ by Epitaxial Strain: Experimental and Theoretical Investigations, J. Phys. Chem. C, 118 (2014), 6448–6453.
7. M.M. Rashad, I.A. Ibrahim, I.Osama, “Distinction between SnO₂ nanoparticles synthesized using Co-precipitation and solvothermal method for the photovoltaic efficiency of dye-sensitized solar cells” Bull. Mater. Sci. 37 (2014) 903-909.
8. G.R.R.A. Kumara, Kenji Murakami, Masaru Shimomura, K. Velauthamurty, E.V.A. Premalal, R.M.G. Rajapakse, H.M.N. Bandara, Electrochemical Impedance and X-Ray Photoelectron Spectroscopic Analysis of Dye-Sensitized Liquid Electrolyte Based SnO₂/ZnO Solar Cell, J. Photochem. Photobiol A 215 (2010) 1-10.
9. K. Tennakone, J. Bandara, P. K. M. Bandaranayake, G. R. A. Kumara, A. Konno, Enhanced Efficiency of a Dye-Sensitized Solar Cell Made from MgO-Coated Nanocrystalline SnO₂, Jpn. J. Appl. Phys. 40 (2001) L732- L734.
10. G. R. R. A. Kumara, K. Tennakone, V. P. S. Perera, A. Konno, S. Kaneko, M. Okuya, Suppression of Recombinations in a Dye-sensitized Photoelectrochemical Cell made from a Film of Tin IV oxide Crystallites Coated with a Thin Layer of Aluminium oxide, J. Phys.D: Appl. Phys. 34 (2001) 868-873.
11. K.A.T. Amalka Perera, G. Anuradha Sepalage, G.R. Asoka Kumara, M. Lal Paranawitharana, R.M. Gamini Rajapakse, H.M.N. Bandara, The Interconnected, CaCO₃ coated SnO₂ Nanocrystalline Dye-sensitized Solar Cell with Superior Performance, Electrochim. Acta 56 (2011) 4135-4138.
12. E. N. Jayaweera, C. S. K. Ranasinghe, G. R. A. Kumara, R. M. G. Rajapakse, Highly Efficient SnO₂/MgO Composite Film-Based Dye-Sensitized Solar Cells Sensitized with N719 and D358 Dyes, Int. J. Nanosci. 13 (2014) 1440006.
13. K. Basu, D. Benetti, H. Zhao, L. Jin, F. Vetrone, A. Vomiero, F. Rosei, “Enhanced photovoltaic properties in dye-sensitized solar cells by surface treatment of SnO₂ photoanodes” Scientific Reports DOI: 10.1038/srep23312.
14. K Tennakone, I.R.M. Kottegoda, L.A.A. De Silva, V.P.S. Perera “The possibility of ballistic electron transport in dye-sensitized semiconductor nanocrystalline particle aggregates” Semi. Sci. Tech. 14 (1999), 975.
15. C. S. K. Ranasinghe, E. N. Jayaweera, G. R. A. Kumara, R. M. G. Rajapakse, B. Onwona-Agyeman, A. G. U. Perera, K. Tennakone, Tin oxide based dye-sensitized solid-state solar cells: surface passivation for suppression of recombination, Mater. Sci. Semicond. Process. 40 (2015) 890–895.
16. C. S. K. Ranasinghe, E. N. Jayaweera G. R. A. Kumara, R. M. G. Rajapakse, H. M. N. Bandara, M. Yoshimura, Low-Cost Dye-Sensitized Solar Cells Based on Interconnected FTO-Activated Carbon Nanoparticulate Counter Electrode Showing High Efficiency, J. Mat.Sci. Eng. A 5 (2015) 361-368.
17. E.N. Jayaweera, G.R.A. Kumara, H.M.T.G. Pitawala, R.M.G. Rajapakse, Nanda Gunawardhana, H.M.N. Bandara, A. Senarathna, C.S.K. Ranasinghe, Hsin-Hui Huang and M. Yoshimura, Vein graphite-based counter electrodes for dye-sensitized solar cells, J. Photochem. Photobiol. (2017), DOI: 10.1016/j.jphotochem.2017.05.00.

Highlights

- Graphene-based counter electrodes are developed.
- These low-cost counter electrodes are used in SnO₂/ZnO composite film based dye-sensitized solar cells.
- A solar to electricity conversion efficiency of 5.5 % is achieved which is comparable to that obtained for the similar system employing expensive Pt-Cr-FTO counter electrodes.